Propellant Bulk Temperature Modeling for the Orion Launch Abort System

Justin Fox[1] and Joseph Bonafede[2]
Orbital Sciences Corporation, Dulles, VA, 20148
ARES Corporation, Dulles, VA, 20148

In support of the Orion Program's Launch Abort System (LAS) development effort, several techniques have been developed and evaluated for estimating the propellant mean bulk temperature (PMBT) of the main abort motor given only external sensor readings. First, an analytic technique involving the use of Duhamel superposition to estimate the propellant's temperature response given the case temperature history as measured by external sensors or to provide bounding estimates given insufficient data was developed. The analytic method was then compared with the results of a Thermal Desktop model whose runtime may preclude it from use in real-time launch operations but which otherwise produces both external case temperature sensor predictions and a bound on the PMBT given just the external environment inputs. The result of this work should enable flight test operators to accurately predict the propellant temperature from available data and make a "go" or "no-go" decision for the upcoming pad abort test of the LAS, the first full-scale test flight in NASA's ambitious efforts to send humanity back to the moon and beyond. This work was conducted by Orbital Sciences Corporation, under the supervision and guidance of Lockheed Martin and NASA thermal analysts.

Nomenclature

Ψ^+, Φ^+ = temperature response to unit step external temperature change

$\Theta+$ = temperature response to unit ramp external temperature change

Φ^+_{sine} = temperature response to unit sinusoidal external temperature change

T = temperature

[1] Orion Lead Systems Thermal Analyst, Orbital, 21839 Atlantic Blvd., Dulles, VA, 20148
[2] Orion Thermal Analyst, ARES Corporation, 21839 Atlantic Blvd, Dulles, VA 20148

θ	=	temperature difference, $T\text{-}T_{init}$
ΔT_{ext}	=	exterior temperature step
$\Delta\theta_{ext}$	=	exterior temperature difference step, $T_{ext}\text{-}T_{init}$
t	=	time
τ_0	=	initial time
r	=	radial dimension
λ	=	eigenvalue
h_{eff}	=	effective exterior heat transfer coefficient
Bi	=	non-dimensional effective heat transfer coefficient, the Biot number
α	=	thermal diffusivity
k	=	thermal conductivity
J_n	=	Bessel function of the first kind of order n
Y_n	=	Bessel function of the second kind of order n
A_n	=	series coefficient for temperature response
B_n	=	series coefficient for bulk temperature response
β	=	ramp rate
ω	=	frequency
ϕ	=	phase
$_o$	=	outer radius
$_i$	=	inner radius
$_{init}$	=	initial condition
$_{ext}$	=	external boundary condition at r_o
$_b$	=	mean bulk temperature
$_{max}$	=	maximum time, for unit ramp external temperature change
$_{lag}$	=	temperature lag function

I. Introduction

ONE of the most satisfying aspects of NASA's bold new manned spaceflight initiative is the emphasis on safety. Nothing exemplifies this commitment more than the design and test of a Launch Abort System tower which, in the event of disaster during launch, will lift the astronauts clear of danger and return them safely to Earth. Of course, propelling the command module clear of a possible explosion requires a rocket engine capable of predictable, reliable, and nearly instantaneous thrust. The main abort motor of the Launch Abort System, designed by a team including Orbital Sciences, NASA, Lockheed Martin, and ATK, will meet these demanding objectives.

To predict the performance of this solid rocket motor, it is important to be able to estimate the propellant mean bulk temperature (PMBT) prior to launch. The PMBT is, of course, a function of the external thermal environments, including ambient air temperature, solar radiation, and sky-radiation sink temperature, as well as the thermophysical and optical properties of the vehicle itself. For the purposes of this paper, we will largely divorce ourselves from a discussion of the external environments by assuming that we are able to accurately sense the temperature of the abort motor case. Therefore, the task at hand is to estimate the propellant mean bulk temperature as quickly and as simply as possible, given a sensor history of the outer case temperature. If possible, the technique developed should be simple enough that launch operators not affiliated with the thermal community can easily use it to make "go-no go" launch predictions on the day of flight.

II. Generalized Description of the Problem

While the exact dimensions and material composition of the abort motor case and propellant are complex and not suitable for open publication, our problem can be generalized to a much simpler state. We will presume that we have an exterior temperature history as a function of time $T_{ext}(r_o,t)$. This temperature will be applied to the outer shell of a hollow cylinder which contains, among other things, the propellant mass. The propellant itself will be modeled as a cylinder having an outer radius r_o and an inner radius r_i. The axial boundaries of the abort motor are modeled as adiabatic in comparison to the radial boundary. Both of these modeling assumptions are amenable to the application at hand.

Given a non-dimensional Biot number, the geometric properties of the system, and the temperature sensor history, the question then becomes simply one of estimating the worst case, or even better, the actual temperature difference between the external sensor measurement and the PMBT. With this information, a launch operator could decide whether or not the PMBT could be guaranteed to be within its operational temperature range based on the measured information.

III. An Analytical Modeling Approach

An analytical solution to the problem is possible with the following assumptions: (1) the exterior temperature function is assumed uniform in space, $T_{ext}(t)$, (2) the thermal properties of the various materials are assumed constant with temperature, (3) the heat capacity of the case materials are assumed negligible relative to the heat capacity of the propellant, and (4) all materials begin at a uniform initial temperature. Together with the axisymmetry of the geometry, the first assumption of uniform external temperature provides for a one-dimensional problem statement in the radial dimension. The second and third assumptions applied to the case materials allow the thermal resistance between the measured exterior temperature and the propellant to be modeled as an effective heat transfer coefficient, h_{eff}. The problem statement is then simplified to the conduction within the propellant along with this effective heat transfer coefficient and the exterior temperature function in the boundary conditions. The fourth assumption is essential to the model derivation but does not need to be approximated in reality provided that a sufficient history of the external temperature function is available in order that the final state of the model is not strongly dependent upon its initial condition. With these assumptions, the analytical problem is stated as:

$$\frac{\partial T(r,t)}{\partial t} = \alpha \frac{1}{r}\frac{\partial}{\partial r}\left(r \frac{\partial T(r,t)}{\partial r} \right)$$

$$\text{For } t \le \tau_0, \quad \mathrm{T} = \mathrm{T_{init}}$$

$$\text{For } r = r_i, \quad -\mathrm{k}\frac{\partial \mathrm{T}}{\partial \mathrm{r}} = 0$$

$$\text{For } r = r_o, \quad -\mathrm{k}\frac{\partial \mathrm{T}}{\partial \mathrm{r}} = h_{eff}\left(T - T_{ext}(t)\right)$$

where

$$T_{ext}(t) = \begin{cases} T_{init} & \text{for } \ t < \tau_0 \\ T_{init} + \Delta T_{ext}(t) & \text{for } \ t \ge \tau_0 \end{cases}$$

The analytical solution for the propellant mean bulk temperature, $T_b(t)$, is found by first using separation of variables to solve for the bulk temperature response to a sudden step external temperature change, ΔT_{ext}, and then using the Duhamel superposition integral to incorporate the time varying outer radial boundary condition.[(1)] To simplify the solution and generalize the results, the following non-dimensional forms are used:

$$\Psi^+(r^+,t^+) = 1-\Phi^+(r^+,t^+) = \frac{T(r^+,t^+)-\left(T_{init}+\Delta T_{ext}\right)}{T_{init}-\left(T_{init}+\Delta T_{ext}\right)} = \frac{T(r^+,t^+)-\left(T_{init}+\Delta T_{ext}\right)}{-\Delta T_{ext}}$$

$$\Phi^+(r^+,t^+) = 1-\Psi^+(r^+,t^+) = \frac{\theta(r^+,t^+)}{\Delta\theta_{ext}} = \frac{T(r^+,t^+)-T_{init}}{\left(T_{init}+\Delta T_{ext}\right)-T_{init}} = \frac{T(r^+,t^+)-T_{init}}{\Delta T_{ext}}$$

$$t^+ = \frac{\left(t-\tau_0\right)\alpha}{r_o^2}$$

$$r^+ = \frac{r}{r_o}$$

$$\lambda_n^+ = \lambda_n r_o$$

$$\mathrm{Bi} = \frac{h_{eff}\, r_o}{k}$$

Using these non-dimensional forms, the temperature and bulk temperature response functions for a unit external temperature change are:

$$\Psi^+(r^+,t^+) = 1-\Phi^+(r^+,t^+) = \sum_{n=1}^{\infty} A_n\left(\mathrm{J}_0(\lambda_n^+ r^+) - \frac{\mathrm{J}_1(\lambda_n^+ r_i^+)}{\mathrm{Y}_1(\lambda_n^+ r_i^+)}\mathrm{Y}_0(\lambda_n^+ r^+)\right)\exp\left(-\lambda_n^{+2} t^+\right)$$

$$\Psi_b^+(t^+) = 1-\Phi_b^+(t^+) = \frac{2}{r_o^{+2}-r_i^{+2}}\int_{x^+=r_i^+}^{x^+=r_o^+}\Psi^+(x^+,t^+)x^+dx^+ = \frac{2r_o^+}{r_o^{+2}-r_i^{+2}}\sum_{n=1}^{\infty}\frac{B_n}{\lambda_n^+}\exp\left(-\lambda_n^{+2}t^+\right)$$

where

$$A_n = \frac{2\Psi_0^+\,\mathrm{Bi}\, r_o^+ Y_1(\lambda_n^+ r_i^+)\left(\mathrm{J}_0(\lambda_n^+ r_o^+)\mathrm{Y}_1(\lambda_n^+ r_i^+)-\mathrm{J}_1(\lambda_n^+ r_i^+)\mathrm{Y}_0(\lambda_n^+ r_o^+)\right)}{\left(\lambda_n^{+2}-\mathrm{Bi}^2\right)r_o^{+2}\left(\mathrm{J}_0(\lambda_n^+ r_o^+)\mathrm{Y}_1(\lambda_n^+ r_i^+)-\mathrm{J}_1(\lambda_n^+ r_i^+)\mathrm{Y}_0(\lambda_n^+ r_o^+)\right)^2-\lambda_n^{+2}r_i^{+2}\left(\mathrm{J}_0(\lambda_n^+ r_i^+)\mathrm{Y}_1(\lambda_n^+ r_i^+)-\mathrm{J}_1(\lambda_n^+ r_i^+)\mathrm{Y}_0(\lambda_n^+ r_i^+)\right)^2}$$

$$B_n = A_n\left(\mathrm{J}_1(\lambda_n^+ r_o^+) - \frac{\mathrm{J}_1(\lambda_n^+ r_i^+)}{\mathrm{Y}_1(\lambda_n^+ r_i^+)}\mathrm{Y}_1(\lambda_n^+ r_o^+)\right)$$

and where λ_{n}^+ are the positive roots of the characteristic equation

$$\mathrm{J}_1(\lambda_n^+ r_i^+)\left(\mathrm{Bi}\,\mathrm{Y}_0(\lambda_n^+ r_o^+)-\lambda_n^+\mathrm{Y}_1(\lambda_n^+ r_o^+)\right)-\mathrm{Y}_1(\lambda_n^+ r_i^+)\left(\mathrm{Bi}\,\mathrm{J}_0(\lambda_n^+ r_o^+)-\lambda_n^+\mathrm{J}_1(\lambda_n^+ r_o^+)\right)=0$$

Using the bulk temperature response to a unit step external temperature change in the Duhamel superposition integral, the solution for the PMBT rise, θ_b, at time t^+ as a function of the external temperature rise history, θ_{ext}, prior to time t^+ is:

$$\theta_b(t^+) = T_b(t^+)-T_{init} = \int_{s^+=\tau_0^+=0}^{s^+=t^+}\theta_{ext}(s^+)\frac{d\Phi_b^+(t^+-s^+)}{dt^+}ds^+ = \frac{2r_o^+}{r_o^{+2}-r_i^{+2}}\int_{s^+=\tau_0^+=0}^{s^+=t^+}\theta_{ext}(s^+)\sum_{n=1}^{\infty}\lambda_n^+B_n\exp\left(-\lambda_n^{+2}\left(t^+-s^+\right)\right)$$

The analytical solution is in the form of an infinite series. To verify the unit step response functions, $\Psi^+(r^+,t^+)$ and $\Psi_b^+(t^+)$, and to test for satisfactory convergence of the series, the unit step response function was calculated in Microsoft Excel and compared to a numerical solution performed using *Thermal Desktop* thermal analysis software by Cullimore and Ring Technologies, inc. Figures 1 and 2 show the comparison using fifty terms in the analytical solution and non-dimensional parameters representative of those for the abort motor. The series converges more rapidly for larger values of t^+ and smaller values of r^+. Nevertheless, even at t^+ equal to zero and r^+ equal to one, for which the correct solution of Ψ^+ is identically 1, the error in the analytical solution using fifty terms is less than 5.3%. The error in the analytical solution for Ψ_b^+ at t^+ equal to zero using fifty terms is less than 0.002%.

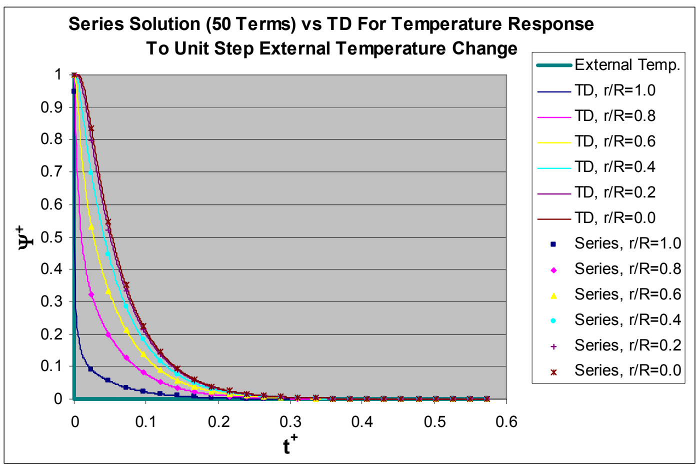

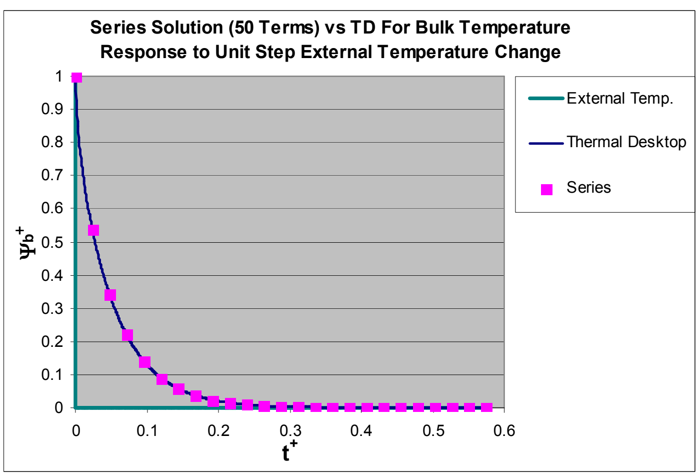

Figures 1 and 2. Comparisons of Temperature and Bulk Temperature Response Functions, Respectively, With Thermal Desktop Results For Unit Step External Temperature Change

Two additional test cases were used to verify the numerical convergence of the Duhamel integral by applying an integrable function for the exterior temperature history. These two test cases also provide valuable insight for estimating bounds on the thermal response of the system. The first of these additional test cases provides the temperature response to a ramp external temperature change. The non-dimensional form and analytical solution for this test case are:

$$\theta_{ext}(t^+) = \begin{cases} 0 & \text{for} \quad t^+ < \tau_0^+ = 0 \\ \left(\dfrac{\partial T_{ext}(t^+)}{\partial t}\dfrac{r_o^2}{\alpha}\right)\left((t-\tau_0)\dfrac{\alpha}{r_o^2}\right) = \beta \mathrm{t}^+ & \text{for} \quad \tau_0^+ \le t^+ \le \mathrm{t}_{\max}^+ \end{cases}$$

$$\Theta^+(r^+,t^+) = \frac{\theta(r^+,t^+)}{\beta t_{\max}^+} = \frac{T(r^+,t^+) - T_{init}}{\beta t_{\max}^+}$$

$$\Theta^+(r^+,t^+) = \sum_{n=1}^{\infty} A_n \left(J_0(\lambda_n^+ r^+) - \frac{J_1(\lambda_n^+ r_i^+)}{Y_1(\lambda_n^+ r_i^+)} Y_0(\lambda_n^+ r^+) \right)\left(\frac{t^+}{t_{\max}^+} - \frac{\left(1 - \exp\left(-\lambda_n^{+2} t^+\right)\right)}{\lambda_n^{+2} t_{\max}^+} \right)$$

$$\Theta_b^+(t^+) = \frac{2r_o^+}{r_o^{+2} - r_i^{+2}} \sum_{n=1}^{\infty} \frac{B_n}{\lambda_n^+} \left(\frac{t^+}{t_{\max}^+} - \frac{\left(1 - \exp\left(-\lambda_n^{+2} t^+\right)\right)}{\lambda_n^{+2} t_{\max}^+} \right)$$

Figures 3 and 4 show the comparison of the analytical and *Thermal Desktop* solutions for the temperature response to a unit ramp external temperature change using non-dimensional parameters representative of those for the abort motor. Fifty terms are used in the analytical solution everywhere except for the solution of $\Theta^+(r_o^+,t^+)$, for which an additional fifty terms are used and yet the solution still does not converge particularly well for larger values of t^+. Using 100 terms and a non-dimension time t^+_{max} of 0.573665, the error in the solution for $\Theta^+(r_o^+,t^+_{max})$, for which the correct solution is identically 1, is less than 4.2%. This test case also illustrates a potential difficulty with the Duhamel integral. The integrand varies exponentially in magnitude over the s^+ interval. For larger values of t^+, numerical difficulties may require special attention, but these difficulties are easily remedied using methods for adaptive step size in the numerical integral.[2]

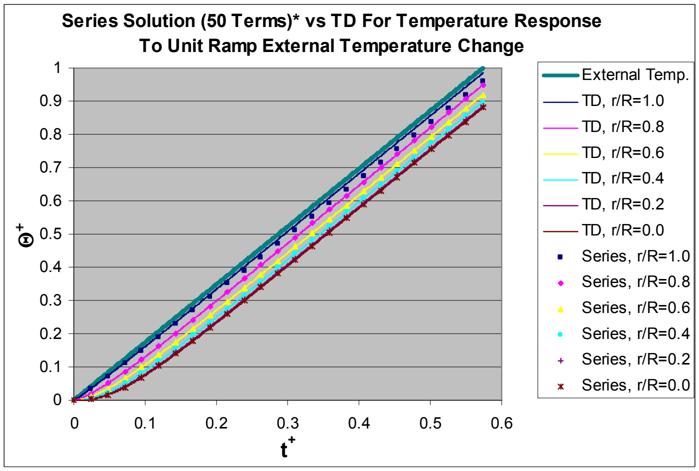

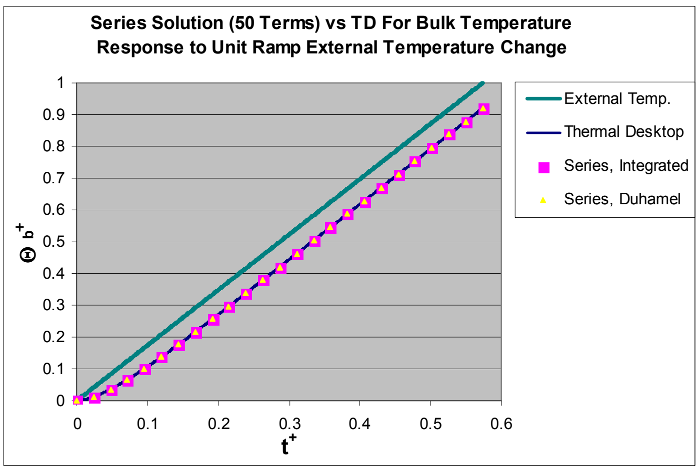

Figures 3 and 4. Comparisons of Temperature and Bulk Temperature Response Functions, Respectively, With Thermal Desktop Results For A Unit Ramp External Temperature Change

Subtracting the external temperature change from these functions provides a solution for the propellant temperature lag when exposed to a ramp external temperature change. The temperature lag is composed of a constant and a transient term. For the non-dimensional parameters used in the above figures, the constant component of the non-dimensional bulk temperature lag is equal to 0.045648, and the non-dimensional time at which 90% of the temperature lag is developed is 0.12297.

$$\Theta^{+}_{lag}(r^{+},t^{+}) = \sum_{n=1}^{\infty} \frac{A_n}{\lambda_n^{+2} t^{+}_{\max}} \left(J_0(\lambda_n^{+} r^{+}) - \frac{J_1(\lambda_n^{+} r_i^{+})}{Y_1(\lambda_n^{+} r_i^{+})} Y_0(\lambda_n^{+} r^{+}) \right) - \sum_{n=1}^{\infty} A_n \left(J_0(\lambda_n^{+} r^{+}) - \frac{J_1(\lambda_n^{+} r_i^{+})}{Y_1(\lambda_n^{+} r_i^{+})} Y_0(\lambda_n^{+} r^{+}) \right) \left(\frac{\exp\left(-\lambda_n^{+2} t^{+}\right)}{\lambda_n^{+2} t^{+}_{\max}} \right)$$

$$\Theta^{+}_{b,lag}(t^{+}) = \frac{2 r_o^{+}}{r_o^{+2} - r_i^{+2}} \sum_{n=1}^{\infty} \frac{B_n}{\lambda_n^{+3} t^{+}_{\max}} - \frac{2 r_o^{+}}{r_o^{+2} - r_i^{+2}} \sum_{n=1}^{\infty} \frac{B_n}{\lambda_n^{+3} t^{+}_{\max}} \exp\left(-\lambda_n^{+2} t^{+}\right)$$

The second additional test case provides the temperature response to a sinusoidal external temperature change. The non-dimensional form and analytical solution for this test case are:

$$\theta_{ext}(t^+) = \begin{cases} 0 & t < \tau_0 \\ \Delta T_{ext} \sin\left(\left(\omega \dfrac{r_o^2}{\alpha}\right)\left(t \dfrac{\alpha}{r_o^2}\right) - \phi_0\right) & \mathrm{t} \geq \tau_0^+ \end{cases}$$

$$\Phi^+_{\sin e}(r^+, t^+) = \frac{T(r^+, t^+) - T_{init}}{\left(T_{init} + \Delta T_{ext}\right) - T_{init}} = \frac{\theta(r^+, t^+)}{\Delta T_{ext}} = \frac{T(r^+, t^+) - T_{init}}{\Delta T_{ext}}$$

$$\Phi^+_{\sin e}(r^+, t^+) = \sum_{n=1}^{\infty} \frac{\lambda_n^{+2} A_n}{\sqrt{\lambda_n^{+4} + \omega^{+2}}} \left(\mathrm{J}_0(\lambda_n^+ r^+) - \frac{\mathrm{J}_1(\lambda_n^+ r_i^+)}{\mathrm{Y}_1(\lambda_n^+ r_i^+)} \mathrm{Y}_0(\lambda_n^+ r^+) \right) \sin\left(\omega^+ t^+ - \phi_0 - \tan^{-1}\left(\frac{\omega^+}{\lambda_n^{+2}}\right)\right)$$
$$+ \sum_{n=1}^{\infty} \frac{\lambda_n^{+2}\left(\lambda_n^{+2} \sin\phi_0 + \omega^+ \cos\phi_0\right) A_n}{\lambda_n^{+4} + \omega^{+2}} \left(\mathrm{J}_0(\lambda_n^+ r^+) - \frac{\mathrm{J}_1(\lambda_n^+ r_i^+)}{\mathrm{Y}_1(\lambda_n^+ r_i^+)} \mathrm{Y}_0(\lambda_n^+ r^+) \right) \exp\left(-\lambda_n^{+2} t^+\right)$$

$$\Phi^+_{b,\sin e}(t^+) = \frac{2 r_o^+}{r_o^{+2} - r_i^{+2}} \sum_{n=1}^{\infty} \frac{\lambda_n^+ B_n}{\sqrt{\lambda_n^{+4} + \omega^{+2}}} \sin\left(\omega^+ t^+ - \phi_0 - \tan^{-1}\left(\frac{\omega^+}{\lambda_n^{+2}}\right)\right)$$
$$+ \frac{2 r_o^+}{r_o^{+2} - r_i^{+2}} \sum_{n=1}^{\infty} \frac{\lambda_n^+\left(\lambda_n^{+2} \sin\phi_0 + \omega^+ \cos\phi_0\right) B_n}{\lambda_n^{+4} + \omega^{+2}} \exp\left(-\lambda_n^{+2} t^+\right)$$

Figures 5 and 6 show the comparison of the analytical and *Thermal Desktop* solutions for the temperature response to a unit sinusoidal external temperature change using non-dimensional parameters representative of those for the abort motor and using fifty terms in the analytical solution. This solution also has a quasi-steady and a transient component with a similar time constant as observed in the temperature response to a ramp external temperature change. For this solution, the quasi-steady component of the non-dimensional bulk temperature has an amplitude and phase lag which can be estimated from the figures below as 0.45 and 315 degrees, respectively, for the given non-dimensional parameters.

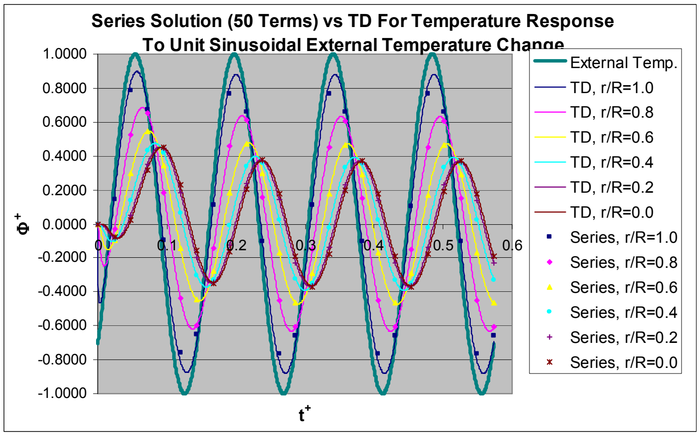

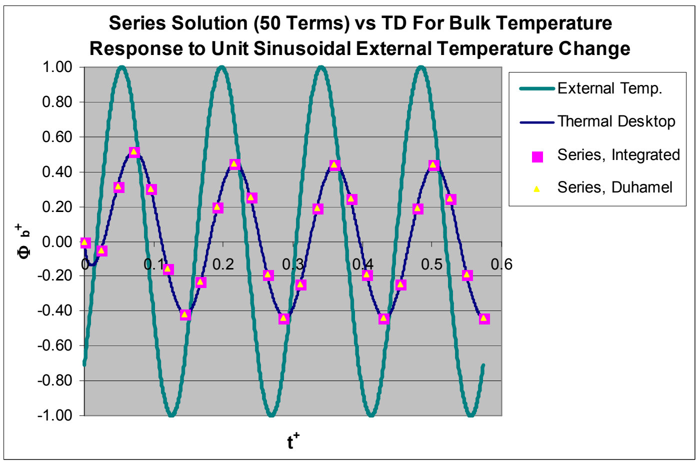

Figures 5 and 6. Comparisons of Temperature and Bulk Temperature Response Functions, Respectively, With Thermal Desktop Results For A Unit Sinusoidal External Temperature Change

This temperature response function can be subtracted from the sinusoidal external temperature change to provide a solution for the propellant temperature lag when exposed to a sinusoidal external temperature change. As expected, the temperature lag function is composed of a constant and a transient term with the constant term characterized by an amplitude ratio and phase change with respect to the external temperature function. As shown in Figure 7, the temperature lag has an amplitude of approximation 0.8 that of the external temperature function and a slight phase lag.

$$\Phi^{+}_{\sin,lag}(r^{+},t^{+}) = \sum_{n=1}^{\infty} \frac{\omega^{+} A_n}{\sqrt{\lambda_n^{+4} + \omega^{+2}}} \left(J_0(\lambda_n^{+} r^{+}) - \frac{J_1(\lambda_n^{+} r_i^{+})}{Y_1(\lambda_n^{+} r_i^{+})} Y_0(\lambda_n^{+} r^{+}) \right) \sin\left(\omega^{+} t^{+} - \phi_0 - \left(\tan^{-1}\left(\frac{\omega^{+}}{\lambda_n^{+2}} \right) - \frac{\pi}{2} \right) \right)$$

$$- \sum_{n=1}^{\infty} \frac{\lambda_n^{+2}\left(\lambda_n^{+2} \sin\phi_0 + \omega^{+} \cos\phi_0\right) A_n}{\lambda_n^{+4} + \omega^{+2}} \left(J_0(\lambda_n^{+} r^{+}) - \frac{J_1(\lambda_n^{+} r_i^{+})}{Y_1(\lambda_n^{+} r_i^{+})} Y_0(\lambda_n^{+} r^{+}) \right) \exp\left(-\lambda_n^{+2} t^{+}\right)$$

$$\Phi^{+}_{b,\sin,lag}(t^{+}) = \frac{2 r_o^{+}}{r_o^{+2} - r_i^{+2}} \sum_{n=1}^{\infty} \frac{\omega^{+} B_n}{\lambda_n^{+} \sqrt{\lambda_n^{+4} + \omega^{+2}}} \sin\left(\omega^{+} t^{+} - \phi_0 - \left(\tan^{-1}\left(\frac{\omega^{+}}{\lambda_n^{+2}} \right) - \frac{\pi}{2} \right) \right)$$

$$- \frac{2 r_o^{+}}{r_o^{+2} - r_i^{+2}} \sum_{n=1}^{\infty} \frac{\lambda_n^{+}\left(\lambda_n^{+2} \sin\phi_0 + \omega^{+} \cos\phi_0\right) B_n}{\lambda_n^{+4} + \omega^{+2}} \exp\left(-\lambda_n^{+2} t^{+}\right)$$

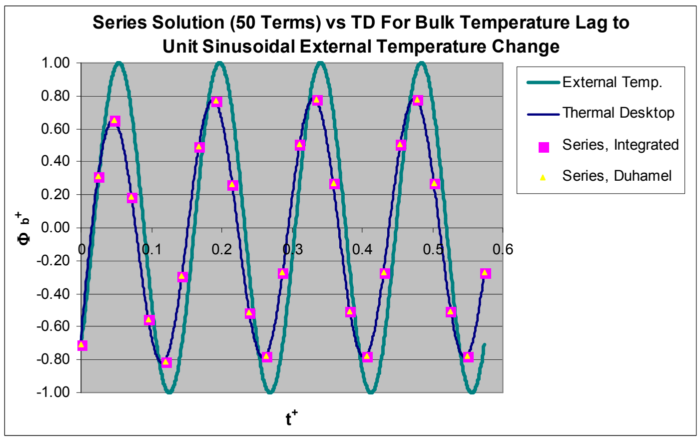

Figure 7. Comparisons of Temperature and Bulk Temperature Lag Functions, Respectively, With Thermal Desktop Results For A Unit Sinusoidal External Temperature Change

IV. A Thermal Desktop Approach

As a method of obtaining an estimate or bounds on the sensor lag relative to the PMBT using only external thermal environment inputs but at the expense of portability and computational time, a Thermal Desktop model of the system was also developed. For this and other purposes, Orbital Sciences developed a relatively detailed LAS system-level thermal model, a portion of which includes several hollow solid-cylinders and surfaces representing the abort motor propellant and its casing as described briefly above. An overview image of this model is shown below in Figure 8. Dimensions and further detail on model properties and creation have been purposely withheld.

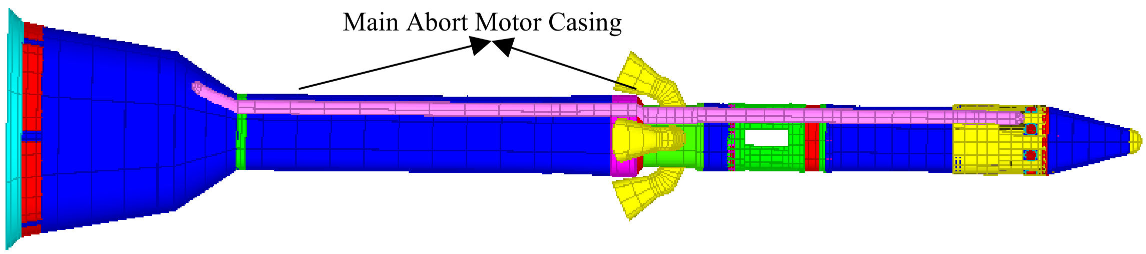

Figure 8. LAS Thermal Desktop System-Level Model

This three-dimensional model was subjected to the worst case natural thermal environments expected during the pre-launch phase of the PA-1 (Pad Abort 1) flight test currently scheduled for March of 2008. For this purpose, the worst case conditions for creating the greatest lag between the sensor reading and the propellant temperature are those combinations that produce either the maximum rate of cooling or heating on the vehicle. If the surface of the vehicle rapidly changes temperature, the propellant bulk and its much larger thermal mass cannot change as quickly, creating the widest possible gap between the sensor and the quantity of importance, the PMBT. In this case, NASA standard environments documents and data collected by Frank Leahy of the NASA Constellation environments working group were used to piece together conditions that would cause the most rapid temperature change physically possible at the White Sands Missile Range launch site. The sensor lag vs. time results are shown below in Figure 9 in non-dimensional temperature units. The two different lines on each plot represent the two sensors which are located at different positions on the motor case, experience different environments, and so tend to read different values.

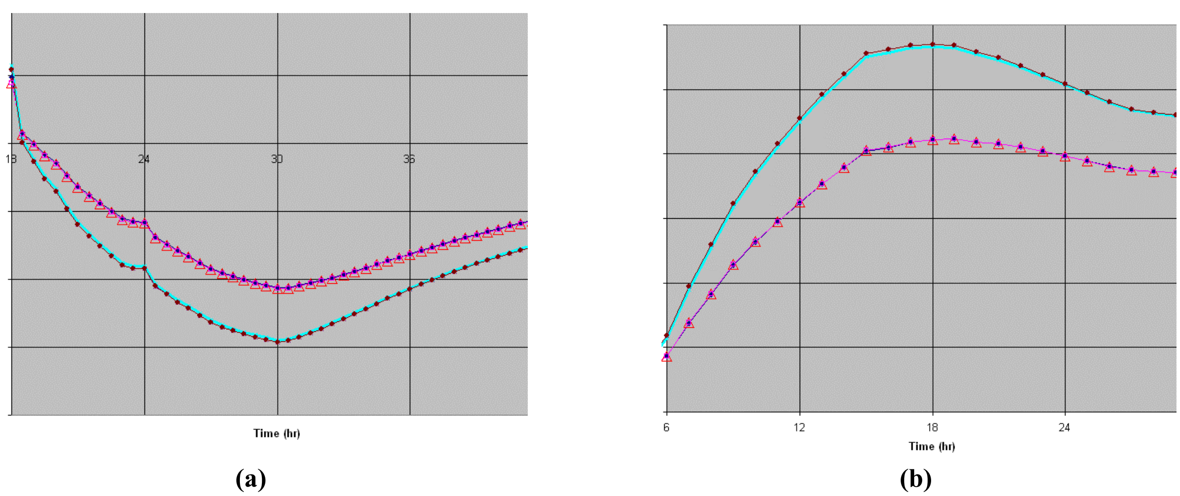

Figure 9. Non-Dimensional Sensor Lag Vs. Time Given Worst Case (a) Cooling and (b) Heating Conditions

What is important to note from these plots is that we can read off of them the absolute worst case difference between the sensors and the PMBT, given the actual three-dimensional geometry of the LAS and accounting for all of the environmental conditions. This yields a tighter bound on the maximum sensor lag than the worst-case estimates from the analytic model for ramp external temperature change discussed in Section III because in reality the sensor temperature cannot maintain a constant maximum slope for extended periods. This model could then give a "go-no go" temperature limit as indicated by the yellow and green sections of the chart in Figure 10. The outer regions are labeled yellow because the analytic model indicates that if the sensor reading is in that range there is a physical chance that the PMBT could conceivably fall outside of an acceptable range. However, unless the environments experienced are worse than those compiled by NASA for the White Sands Missile Range, the computational model indicates that such an event is improbable.

In addition to this worst case bound, a similar Thermal Desktop model also could allow day-of-flight operators to input past sensor data and receive as output the predicted PMBT. Such a tool could provide even more accurate predictions to the ground crew in cases where the maximum sensor lag calculated above would be overly-conservative. One drawback inherent to such a method is that the runtime of even a simplified model could be as much as half an hour, precluding perfectly real-time predictions. However, hourly updates to the "go-no go" PMBT temperature predictions could conceivably allow a widening of the yellow "GO" region of Figure 10.

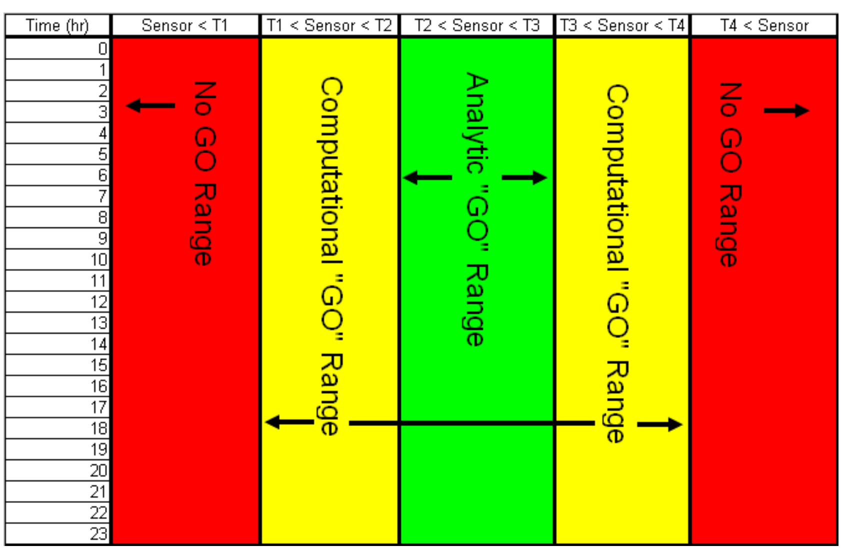

Figure 10. Illustration of Chart Which Could Be Given to Day-Of-Flight Operators Showing the Range of Sensor Temperatures For Which The PMBT is Known To Be Within An Acceptable Range.

V. Conclusion

Accurate prediction of the PMBT from sensors on the outer case of the main Launch Abort System abort motor could help extend the launch capability of the vehicle. Two models have been presented which attempt to perform that prediction. The analytic model provides estimates given the time history of the measured exterior case temperatures, and it can be used to provide worst-case estimates if only an incomplete history of the measured exterior case temperatures is available. The computational model sacrifices a small amount of certainty by incorporating past environmental data in order to provide a limiting-case analysis of the vehicle's launch capability. In the coming months it will be up to the Flight Test Office's operations team to decide upon which model to rely. Orbital's thermal analysts and the rest of the Orion thermal working group will continue working to provide the most reliable and accurate information possible to ensure a successful launch of the PA-1 test article and beyond.

Acknowledgments

The authors would like to thank the NASA, Lockheed Martin, and ATK members of the Orion thermal working group for their invaluable support, advice, and critique throughout the course of this work. Thanks also to Orbital Sciences Corporation and the ARES Corporation for funding the submission of this report.

References

[1] Arpaci, V. S., *Conduction Heat Transfer, Abridged Edition*, Simon & Schuster Custom Publishing, Needham Heights, Massachusetts, 1991, Chap. 5.

[2] Press, W. H., Flannery, B. P., Teukolsky, S. A., and Vetterling, W. T., *Numerical Recipes in C; The Art Of Scientific Computing*, Cambridge University Press, New York, 1988.